Supplementary Data for:

Interplay of DNA damage and cell cycle signaling at the level of human Replication Protein A

Gloria E.O. Borgstahl[1]*, Kerry Brader[1], Adam Mosel[2], Shengqin Liu[2], Elisabeth Kremmer[5], Kaitlin A. Goettsch[3], Carol Kolar[1], Heinz-Peter Nasheuer[4] and Greg G. Oakley[2]

[1]Eppley Institute for Research in Cancer and Allied Diseases, University of Nebraska Medical Center, Omaha, NE, 68198, USA

[2]Department of Oral Biology, University of Nebraska Medical Center, Omaha, NE, 68583, USA

[3]School of Interdisciplinary Informatics, College of Information Science and Technology, University of Nebraska at Omaha, Omaha, NE, 68182, USA

[4]Centre for Chromosome Biology, School of Natural Sciences, National University of Ireland, Galway, Ireland

[5]Institute for Molecular Immunology, Helmholtz Zentrum München, German Research Center for Environmental Health (GmbH), 81377 München, Germany

* To whom correspondence should be addressed. Tel: +1-402-559-8578; Fax: +1-402-559-3739; Email: gborgstahl@unmc.edu

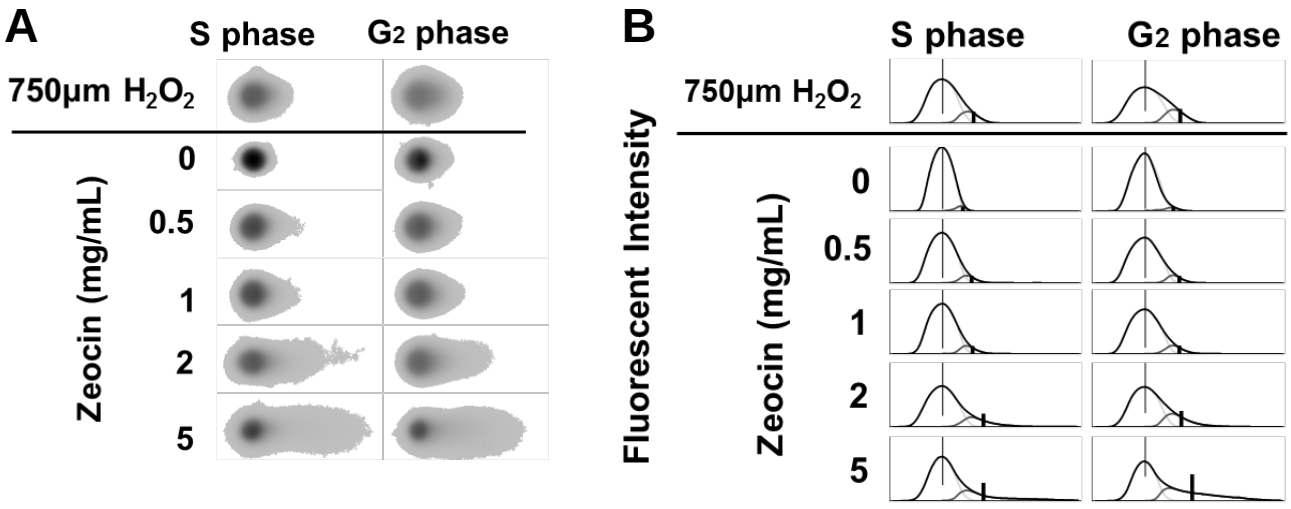

Supplementary Figure S1. Visualizing Zeocin induced double-strand breaks using a modified neutral comet assay. **(A)** Composite images of 75 cells per sample after normalization for total fluorescent intensity where UM-SCC-38 expressing WT RPA2 cells were treated with Zeocin. **(B)** Comet profiles of composite images (thin vertical bar = %DNA in head; thick vertical bar = %DNA in Tail; distance between thin and thick vertical bars represents tail length; black curve = average comet profile; light grey curve = DNA in head; dark grey curve = DNA in tail).

Individual comet images were normalized for total fluorescent intensity, thereby making each comet image directly comparable in terms of %DNA content and subsequent Olive tail moment (%DNA in tail x tail length). Normalization does not affect the tail length values. The 75 normalized images (comets) for each sample were then averaged into their respective composite image. The composite image and its comet profile (all of which have the same area under the curve) directly reflects the average Olive tail moment for that sample.

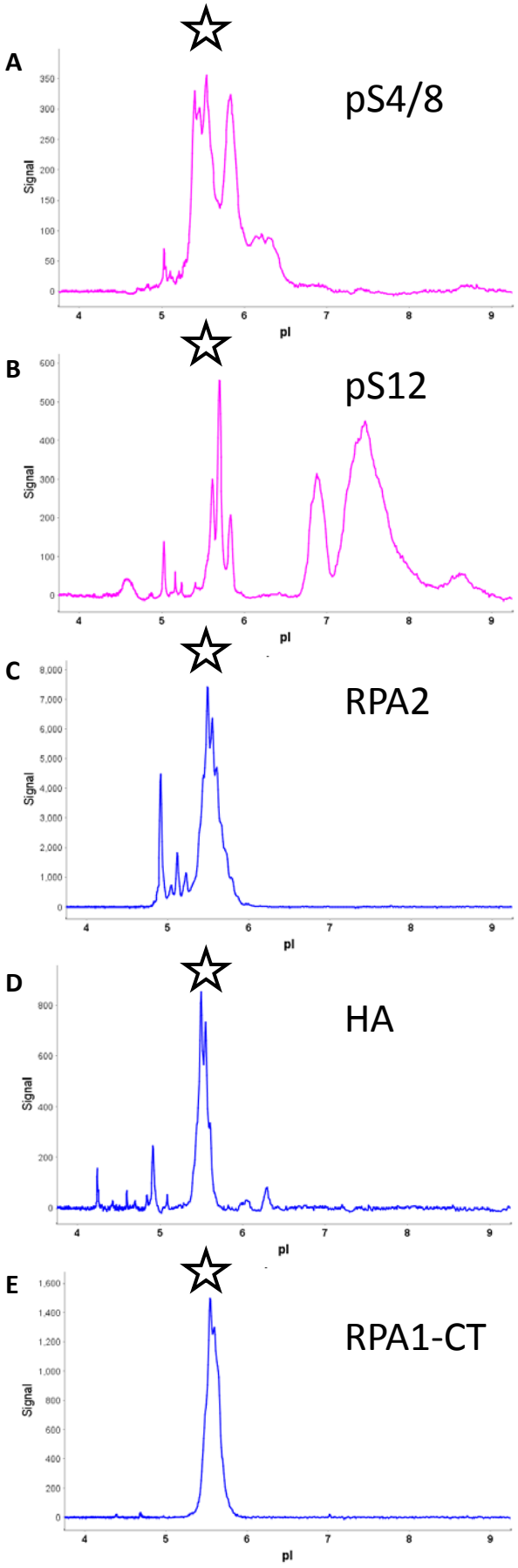

Supplementary Figure S2 . Identification of capillary IEF immunoassay peaks specific for RPA G2 isoforms. Peggy data on a pH 3-10 gradient from several RPA antibodies: (A) pS4/8 antibody (Bethyl) diluted 1:50; (B) pS12 antibody diluted 1:50; (C) RPA2 antibody (Bethyl) diluted 1:500; (D) HA antibody (Neomarkers) diluted 1:25; (E) RPA1-CT antibody not diluted. In parts A and B, DNA-damaged lysates are shown (t1, pink line). In parts C, D and E control lysates that were not treated are shown (blue line). A star indicates the peaks that are in common for all antibodies and are specific for RPA isoforms under these experimental conditions.

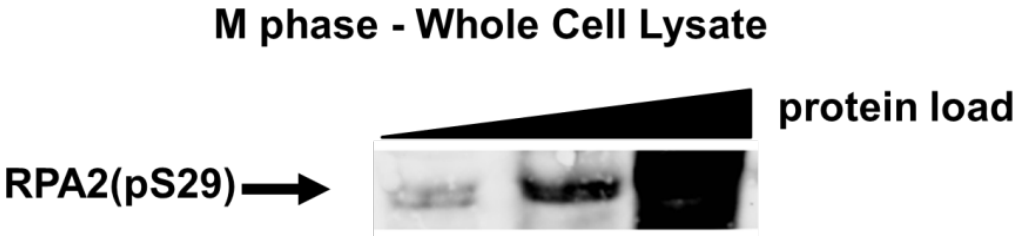

Supplementary Figure S3. To make sure the RPA2(pS29) antibody was active we tested against mitotic cell lysates as a positive control. UM-SCC-38 WT RPA cells synchronized to M phase with nocodazole were harvested and lysed. Whole cell lysate was separated on a 10% Bis-Tris SDS PAGE gel. Proteins were transferred to a nitrocellulose membrane and probed with anti-RPA2(pS29). Protein loaded left to right: 10 µg, 20 µg, 40 µg. Thus, the antibody sample is good and the lack of signal in the westerns is due to very low levels of RPA2(pS29).

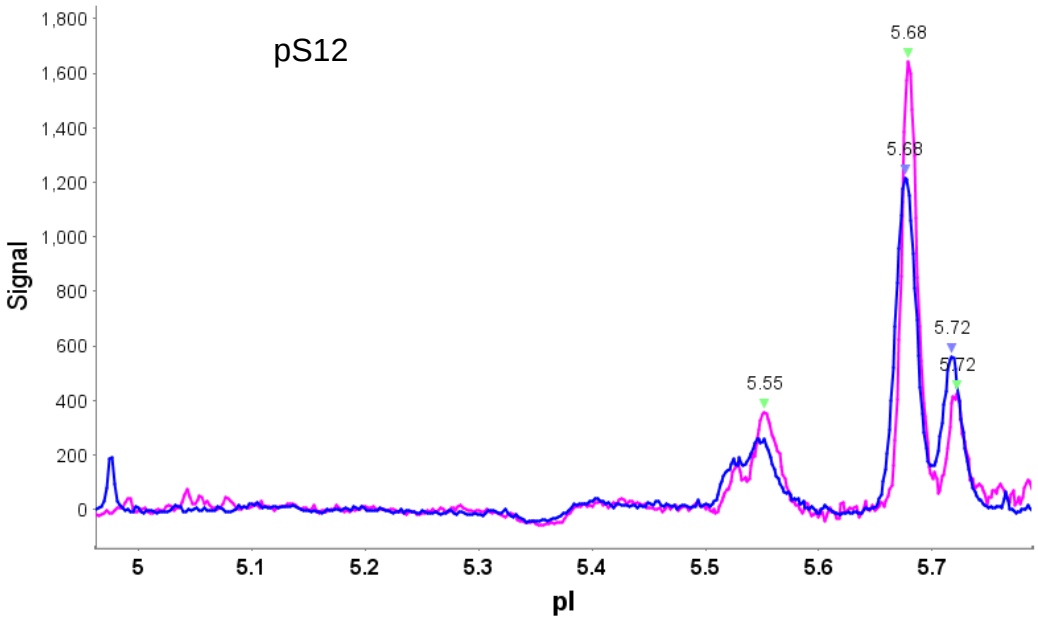

Supplementary Figure S4. Capillary isoelectric focusing data for RPA2 pSer12 antibody. This antibody does not appear to work well with native protein. , DNA-damaged (t1, pink line) and control lysates that were not treated (blue line) are shown.

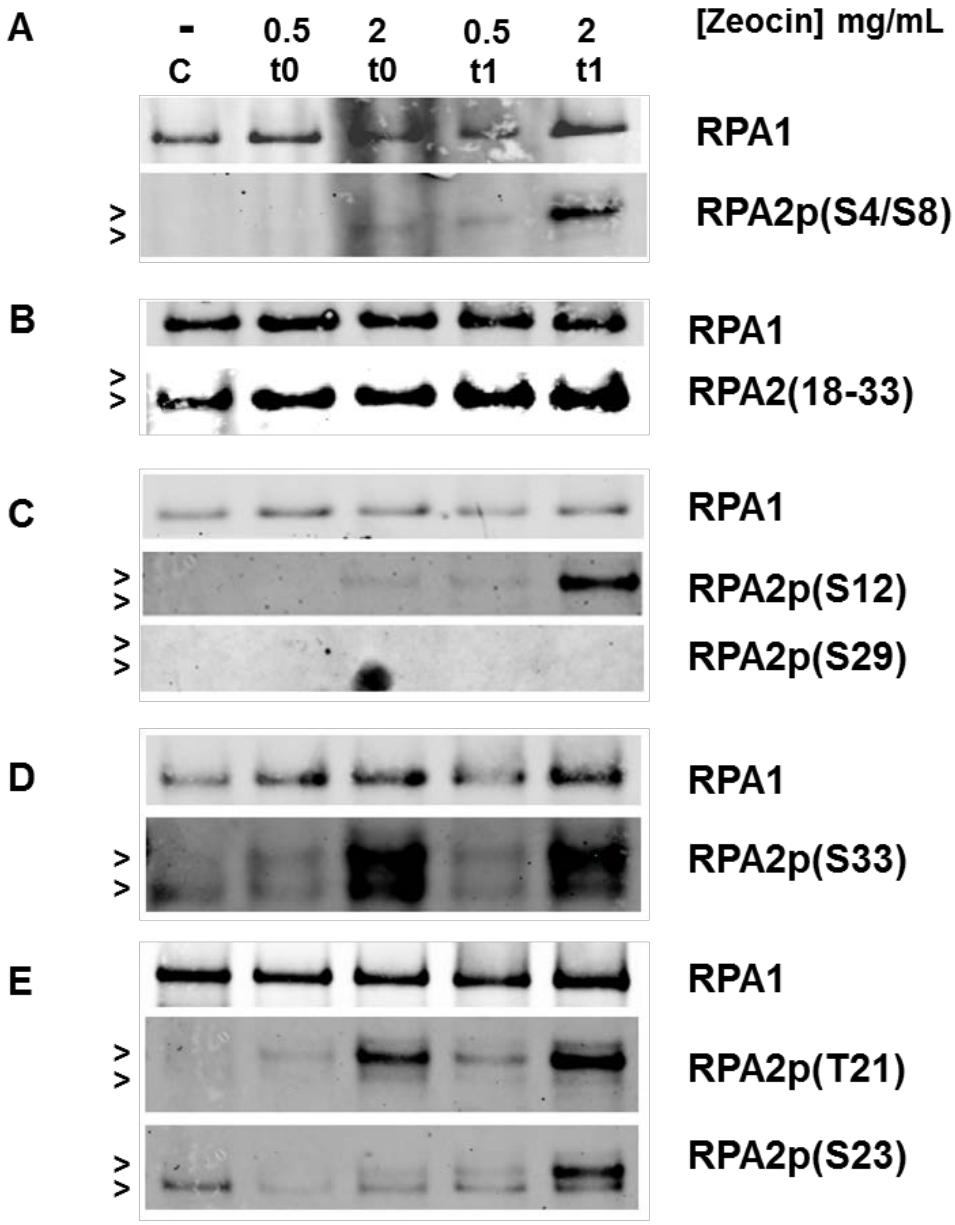

Supplementary Figure S5. Western blots of S phase HA-RPA2 IP of chromatin-bound fraction with respective RPA1 controls. Correlating to **Figure 4B** in the paper.

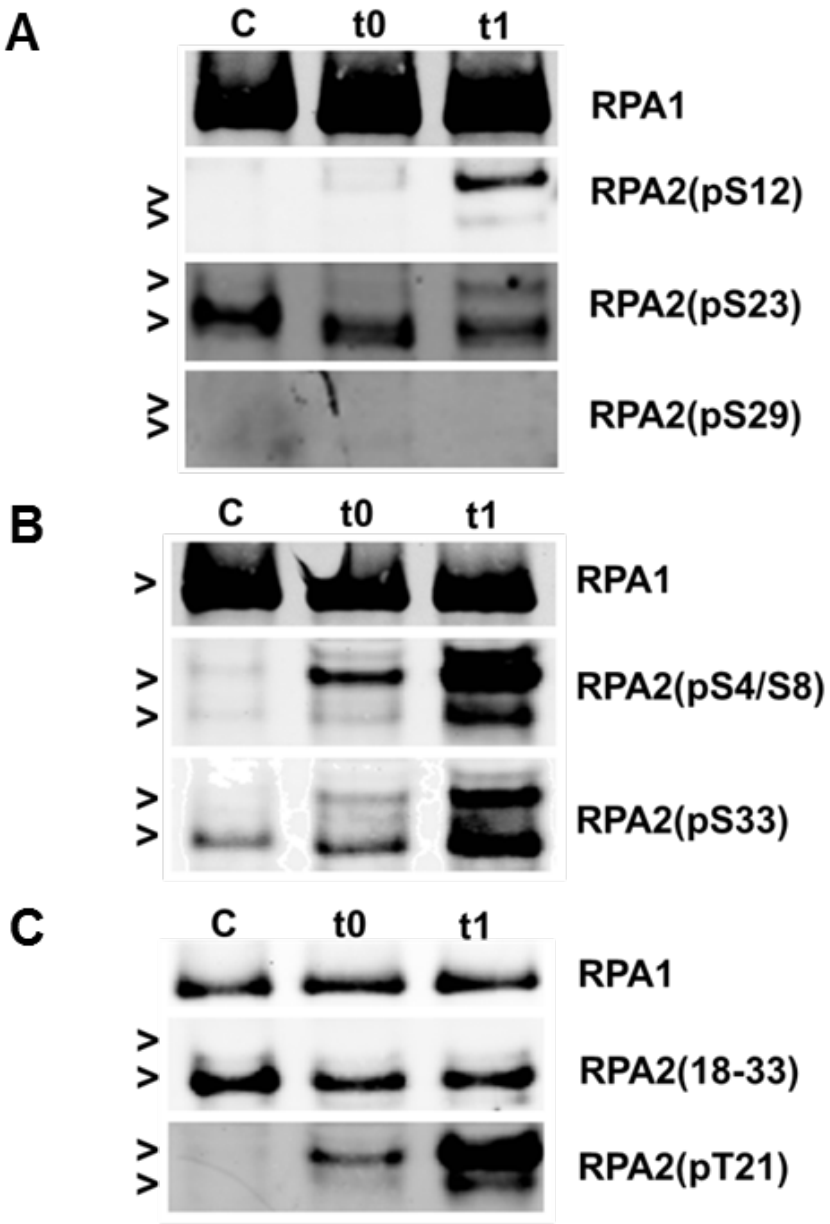

Supplementary Figure S6. Western blots of G2 phase HA-RPA2 IP of chromatin-bound fraction with respective RPA1 controls. Correlating to **Figure 4C** in the paper.

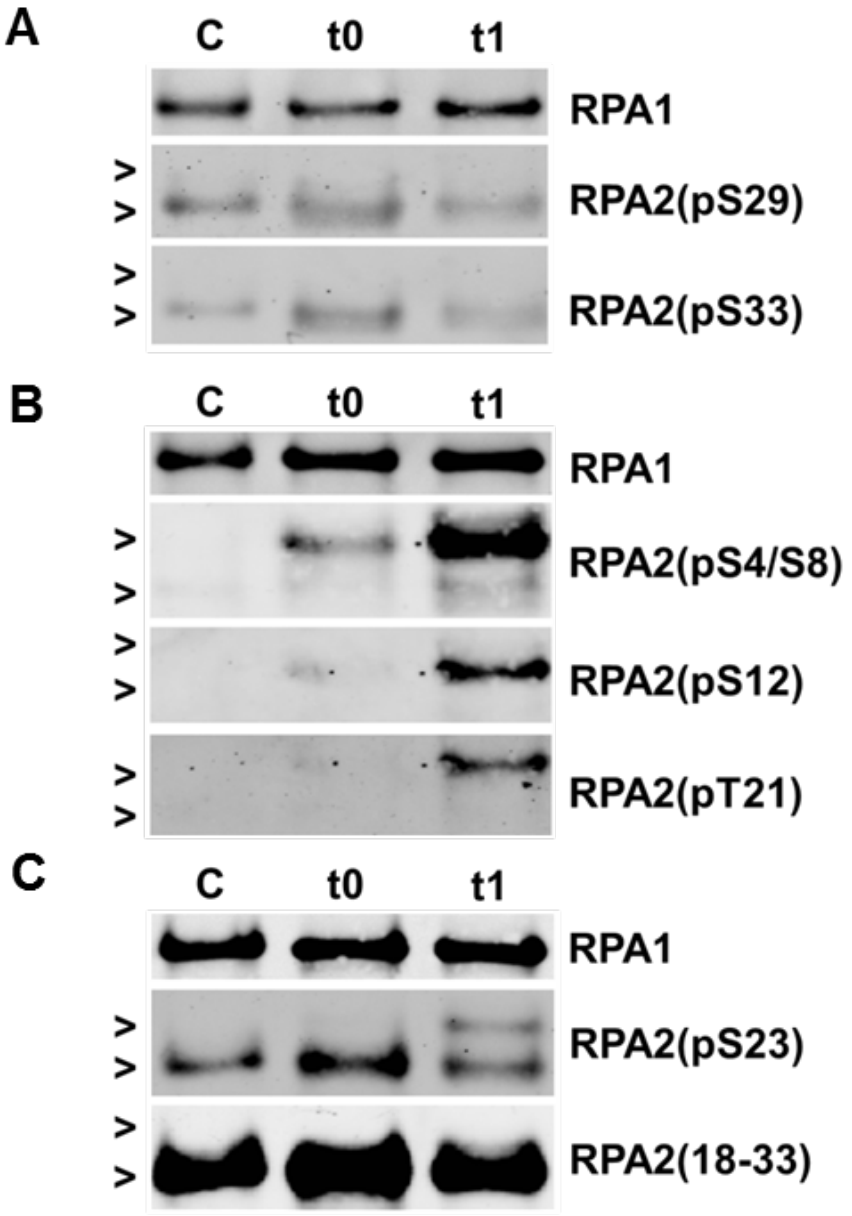

Supplementary Figure S7. Western blots of S phase HA-RPA2 IP of cytosolic fraction with respective RPA1 controls. Correlating to **Figure 5A** in the paper.

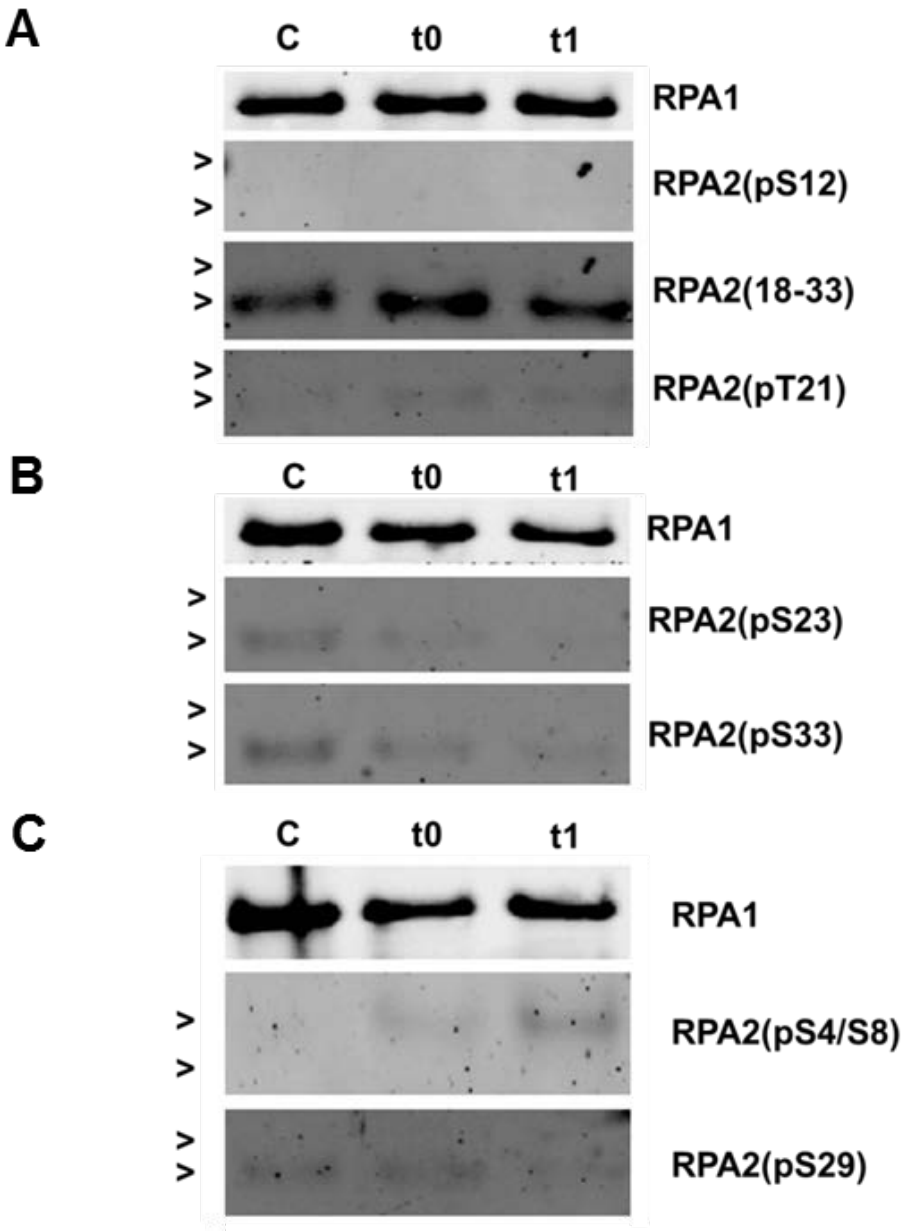

Supplementary Figure S9. Western blots of G2 phase HA-RPA2 IP of cytosolic fraction with respective RPA1 controls. Correlating to **Figure 5B** in the paper.

Table S1. PIKK and CDK phosphorylation sites of human RPA.

Protein	Residue	sequence	Kinase	Cell cycle	Treatment	Ab available?	Reference
RPA1	Ser 38	TTGN**S**PPRY	CK1, CDK	ayn	none	No	[1, 2]
	Thr 180	TSGG**T**QSKV	PIKK, CK1	asyn	IR, UV, none	No	[3-5]
	Ser 207	VTNK**S**QIRT	PIKK	asyn	PMA	No	[6]
	Thr 483	QACP**T**QDCN	PIKK	asyn	none	No	[7]
RPA2	Ser 4,8	MWN**S**GFE**S**YGSS	PIKK	S, asyn, M	UV, HU, IR, ETOP	Yes	[8-11]
	Ser 11,12,13	ESYG**SSS**YGGA	PIKK	asyn, M	UV, none, ETOP	Yes	[9, 11, 12]
	Thr 21	AGGY**T**QSPG	PIKK, CHK2	S, asyn	UV, HU, IR, CPT, ETOP	Yes	[8, 9, 11, 13, 14]
	Ser 23	GYTQ**S**PGGF	CDK	S/G2, M, asyn	IR, UV	Yes	[9, 10, 12, 15]
	Ser 29	GGFG**S**PAPS	CDK	S/G2, M, asyn	IR, UV	Yes	[9, 10, 13, 15, 16]
	Ser 33	SPAP**S**QAEK	PIKK	asyn, S	UV, HU, ETOP	Yes	[8, 9, 11, 13, 14]
	Ser 52	PCTI**S**QLLS	PIKK/GSK3	*in vitro*	None	No	[8]
	Ser 72	NVEI**S**QVTI	PIKK	*in vitro*	None	No	[8]
	Ser 174	SKAN**S**QPSA	PIKK	*in vitro*	None	No	[8]

Treatments: CPT = camptothecin; ETOP = etoposide; HU=hydroxyurea; IR=ionizing radiation; PMA = phorbol 12-myristate 13-acetate

Kinase: PIKK = ATM/ATR or DNA-PKcs; CDK = cyclin dependent kinase; CHK = checkpoint homolog kinase, CK = casein kinase, GSK = glycogen synthase kinase

Table S2. Other phosphorylation sites of human RPA.

Sub-unit	Residue	Sequence	Kinase[a]	Reference
RPA1	Ser 6	VGQL**S**EGAI		[1, 5, 17]
	Thr 34,35	IRPI**TT**GNSP	CAMK2	[17]
	Ser 135	APAA**S**PAAS	GSK3	[17, 18]
	Ser 174	GPSL**S**HTSG		[1, 2]
	Ser 177	LSHT**S**GGTQ	CK1	[1]
	Ser 182	GGTQ**S**KVVP		[1]
	Thr 191	IASL**T**PYQS		[2, 5, 18-20]
	Ser 315	KSKD**S**LVDI	CK1, Aurora	[1, 19]
	Ser 371	KFDG**S**RQPV		[1]
	Ser 384	GARV**S**DFGG	PKA	[1, 5, 6, 12, 17]
	Ser 432	SDLK**S**GGVG	CK1	[17]
	Ser 438	GVGG**S**NTNW	PKA	[5, 6, 12]
	Thr 440	GGSN**T**NWKT		[17]
	Tyr 461	DKPD**Y**FSSV		[1]
	Ser 463,464	PDYF**SS**VATV		[17]
	Thr 467	SSVA**T**VVYL	CK1	[17]
	Tyr 470	ATVV**Y**LRKE		[17]
	Tyr 478	ENCM**Y**QACP		[1, 7]
	Ser 569	ANFR**S**FIFR		[18]
	Thr 580	VKVE**T**YNDE		[18]
	Tyr 581	KVET**Y**NDES	EGFR	[1]
	Ser 585	YNDE**S**RIKA		[17, 18]
	Thr 590	RIKA**T**VMDV	Aurora	[1, 5, 18]
	Tyr 599	KPVD**Y**REYG		[1, 5]
RPA2	Tyr 9	GFES**Y**GSSS		[1, 21]
	Ser 39	AEKK**S**RARA		[1, 12, 22]
	Thr 75	ISQV**T**IVGI	CK1	[17]
	Thr 88	EKAP**T**NIVY		[1, 6]
	Thr 98	IDDM**T**AAPM		[18]
	Ser 238	LKHM**S**VSSI		[17]
	Ser 241	MSVS**S**IKQA	CK1	[1]

RPA3	Ser 10	DLPR**S**RINA	NEK6	[1]
	Thr 37	KIHP**T**GKMF		[1]
	Ser 44	MFIL**S**DGEG	CK2	[1, 23]
	Thr 52	GKNG**T**IELM		[1, 23]

[a]PHOSIDA Kinase Motif Matcher: CAMK2 = Ca2+/calmodulin-dependent protein kinase, CK = casein kinase, EGFR = epidermal growth factor receptor, GSK = glycogen synthase kinase, NEK = NIMA('never in mitosis A')-related kinase, PKA = protein kinase A

Table S3. Primary antibodies, source and dilutions used

Antibody	Source	Host	Traditional western	Capillary IEF
ATM	Abcam ab17995	Rabbit	1:1000	
pATM(pSer1981)	Abcam ab81292	Rabbit	1:1000	
CHK1 (G-4)	Santa Cruz sc-8408	Mouse	1:3000	
pCHK1(pSer345)	Cell Signaling #2341	Rabbit	1:500	
CHK2	Abcam ab47433	Rabbit	1:1000	
pCHK2(pThr68)	Abcam ab38461	Rabbit	1:1000	
H2AX	Cell Signaling #2595	Rabbit	1:1000	
γH2AX(pS139)	Abcam ab2893	Rabbit	1:1000	
Actin, N-terminal	Sigma A2103	Rabbit	1:1000	
α-tubulin (10D8)	Santa Cruz sc-53646	Mouse	1:2000	
RPA1 (RPA70-9)	Millipore NA13	Mouse	1:1000	
RPA1(aa 525-616)[a]	Nasheuer lab RAC-4D9 [24]	Rat		No dilution
RPA2 (aa 225-270)	Bethyl A300-244A	Mouse		1:500
pRPA2(pSer4/Ser8)	Abcam87277	Rabbit	1:1000	
	Bethyl A300-245A	Rabbit		1:50
pRPA2(pSer12)	Oakley lab	Rabbit	1:3000	1:50
pRPA2(pThr21)	Abcam ab61065	Rabbit	1:1000	1:25
pRPA2(pSer23)	Nasheuer lab RPA1-8H3 [10]	Rat	1:5	No dilution
PRPA2(pSer29)	Nasheuer lab RPA2-8C7	Rat	1:2	No dilution
pRPA2(pSer33)	Abcam ab87278 [10]	Rabbit	1:1000	
	Bethyl A300-246A	Rabbit		1:25
RPA2(aa 18-33 not phospho)	Nasheuer lab RPA-3A2	Rat	1:5	No dilution
Hemaglutinin (HA Ab1)	Thermo Scientific RB-1438	Rabbit		1:25

[a] aa = amino acids

Supplementary References

1. P.V. Hornbeck, J.M. Kornhauser, S. Tkachev, B. Zhang, E. Skrzypek, B. Murray, V. Latham, and M. Sullivan, PhosphoSitePlus: a comprehensive resource for investigating the structure and function of experimentally determined post-translational modifications in man and mouse, Nucleic Acids Res. 40 (2012) D261-70.
2. H. Zhou, S. Di Palma, C. Preisinger, M. Peng, A.N. Polat, A.J. Heck, and S. Mohammed, Toward a comprehensive characterization of a human cancer cell phosphoproteome, J Proteome Res 12 (2013) 260-71.
3. S. Matsuoka, B.A. Ballif, A. Smogorzewska, E.R. McDonald, 3rd, K.E. Hurov, J. Luo, C.E. Bakalarski, Z. Zhao, N. Solimini, Y. Lerenthal, Y. Shiloh, S.P. Gygi, and S.J. Elledge, ATM and ATR substrate analysis reveals extensive protein networks responsive to DNA damage, Science 316 (2007) 1160-6.
4. M.P. Stokes, J. Rush, J. Macneill, J.M. Ren, K. Sprott, J. Nardone, V. Yang, S.A. Beausoleil, S.P. Gygi, M. Livingstone, H. Zhang, R.D. Polakiewicz, and M.J. Comb, Profiling of UV-induced ATM/ATR signaling pathways, Proc. Natl. Acad. Sci. USA 104 (2007) 19855-60.
5. J.V. Olsen, M. Vermeulen, A. Santamaria, C. Kumar, M.L. Miller, L.J. Jensen, F. Gnad, J. Cox, T.S. Jensen, E.A. Nigg, S. Brunak, and M. Mann, Quantitative phosphoproteomics reveals widespread full phosphorylation site occupancy during mitosis, Sci. Signal. 3 (2010) ra3.
6. K.T. Rigbolt, T.A. Prokhorova, V. Akimov, J. Henningsen, P.T. Johansen, I. Kratchmarova, M. Kassem, M. Mann, J.V. Olsen, and B. Blagoev, System-wide temporal characterization of the proteome and phosphoproteome of human embryonic stem cell differentiation, Sci. Signal. 4 (2011) rs3.
7. Y. Bai, J. Li, B. Fang, A. Edwards, G. Zhang, M. Bui, S. Eschrich, S. Altiok, J. Koomen, and E.B. Haura, Phosphoproteomics identifies driver tyrosine kinases in sarcoma cell lines and tumors, Cancer Res 72 (2012) 2501-11.
8. E. Olson, C.J. Nievera, V. Klimovich, E. Fanning, and X. Wu, RPA2 is a direct downstream target for ATR to regulate the S-phase checkpoint, The Journal of biological chemistry 281 (2006) 39517-33.
9. M. Zernik-Kobak, K. Vasunia, M. Connelly, C.W. Anderson, and K. Dixon, Sites of UV-induced Phosphorylation of the p34 Subunit of Replication Protein A from HeLa Cells, J. Biol. Chem. 272 (1997) 23896-23904.
10. H. Stephan, C. Concannon, E. Kremmer, M.P. Carty, and H.P. Nasheuer, Ionizing radiation-dependent and independent phosphorylation of the 32-kDa subunit of replication protein A during mitosis, Nucleic Acids Res. 37 (2009) 6028-41.
11. S. Liu, S.O. Opiyo, K. Manthey, J.G. Glanzer, A.K. Ashley, C. Amerin, K. Troksa, M. Shrivastav, J.A. Nickoloff, and G.G. Oakley, Distinct roles for DNA-PK, ATM and ATR in RPA phosphorylation and checkpoint activation in response to replication stress, Nucleic Acids Res. 40 (2012) 10780-94.
12. N. Dephoure, C. Zhou, J. Villen, S.A. Beausoleil, C.E. Bakalarski, S.J. Elledge, and S.P. Gygi, A quantitative atlas of mitotic phosphorylation, Proc. Natl. Acad. Sci. USA 105 (2008) 10762-7.
13. H. Niu, H. Erdjument-Bromage, Z.Q. Pan, S.H. Lee, P. Tempst, and J. Hurwitz, Mapping of amino acid residues in the p34 subunit of human single-stranded DNA-binding protein phosphorylated by DNA-dependent protein kinase and Cdc2 kinase in vitro, J. Biol. Chem. 272 (1997) 12634-41.
14. W.D. Block, Y. Yu, and S.P. Lees-Miller, Phosphatidyl inositol 3-kinase-like serine/threonine protein kinases (PIKKs) are required for DNA damage-induced

phosphorylation of the 32 kDa subunit of replication protein A at threonine 21, Nucleic Acids Res. 32 (2004) 997-1005.
15. V.F. Liu and D.T. Weaver, The ionizing radiation-induced Replication Protein A phosphorylation response differs between ataxia telangiectasia and normal human cells, Mol. Cell. Biol. 13 (1993) 7222-7231.
16. F. Fang and J.W. Newport, Distinct roles of cdk2 and cdc2 in RP-A phosphorylation during the cell cycle, J. Cell Sci. 106 (Pt 3) (1993) 983-94.
17. F. Gnad, J. Gunawardena, and M. Mann, PHOSIDA 2011: the posttranslational modification database, Nucleic Acids Res. 39 (2011) D253-60.
18. J.E. Nuss, S.M. Patrick, G.G. Oakley, G.M. Alter, J.G. Robison, K. Dixon, and J.J. Turchi, DNA damage induced hyperphosphorylation of replication protein A. 1. Identification of novel sites of phosphorylation in response to DNA damage, Biochemistry 44 (2005) 8428-37.
19. T. Shiromizu, J. Adachi, S. Watanabe, T. Murakami, T. Kuga, S. Muraoka, and T. Tomonaga, Identification of missing proteins in the neXtProt database and unregistered phosphopeptides in the PhosphoSitePlus database as part of the Chromosome-centric Human Proteome Project, J Proteome Res 12 (2013) 2414-21.
20. S. Gauci, A.O. Helbig, M. Slijper, J. Krijgsveld, A.J. Heck, and S. Mohammed, Lys-N and trypsin cover complementary parts of the phosphoproteome in a refined SCX-based approach, Anal. Chem. 81 (2009) 4493-501.
21. A.B. Iliuk, V.A. Martin, B.M. Alicie, R.L. Geahlen, and W.A. Tao, In-depth analyses of kinase-dependent tyrosine phosphoproteomes based on metal ion-functionalized soluble nanopolymers, Mol Cell Proteomics 9 (2010) 2162-72.
22. E.L. Huttlin, M.P. Jedrychowski, J.E. Elias, T. Goswami, R. Rad, S.A. Beausoleil, J. Villen, W. Haas, M.E. Sowa, and S.P. Gygi, A tissue-specific atlas of mouse protein phosphorylation and expression, Cell 143 (2010) 1174-89.
23. V. Mayya, D.H. Lundgren, S.I. Hwang, K. Rezaul, L. Wu, J.K. Eng, V. Rodionov, and D.K. Han, Quantitative phosphoproteomic analysis of T cell receptor signaling reveals system-wide modulation of protein-protein interactions, Sci. Signal. 2 (2009) ra46.
24. P.E. Pestryakov, K. Weisshart, B. Schlott, S.N. Khodyreva, E. Kremmer, F. Grosse, O.I. Lavrik, and H.P. Nasheuer, Human replication protein A. The C-terminal RPA70 and the central RPA32 domains are involved in the interactions with the 3'-end of a primer-template DNA, J. Biol. Chem. 278 (2003) 17515-24.